O_2 Production Hot Paper

International Edition: DOI: 10.1002/anie.201510156
German Edition: DOI: 10.1002/ange.201510156

Ca^{2+}-Induced Oxygen Generation by FeO_4^{2-} at pH 9–10

Li Ma, William W. Y. Lam, Po-Kam Lo, Kai-Chung Lau, and Tai-Chu Lau**

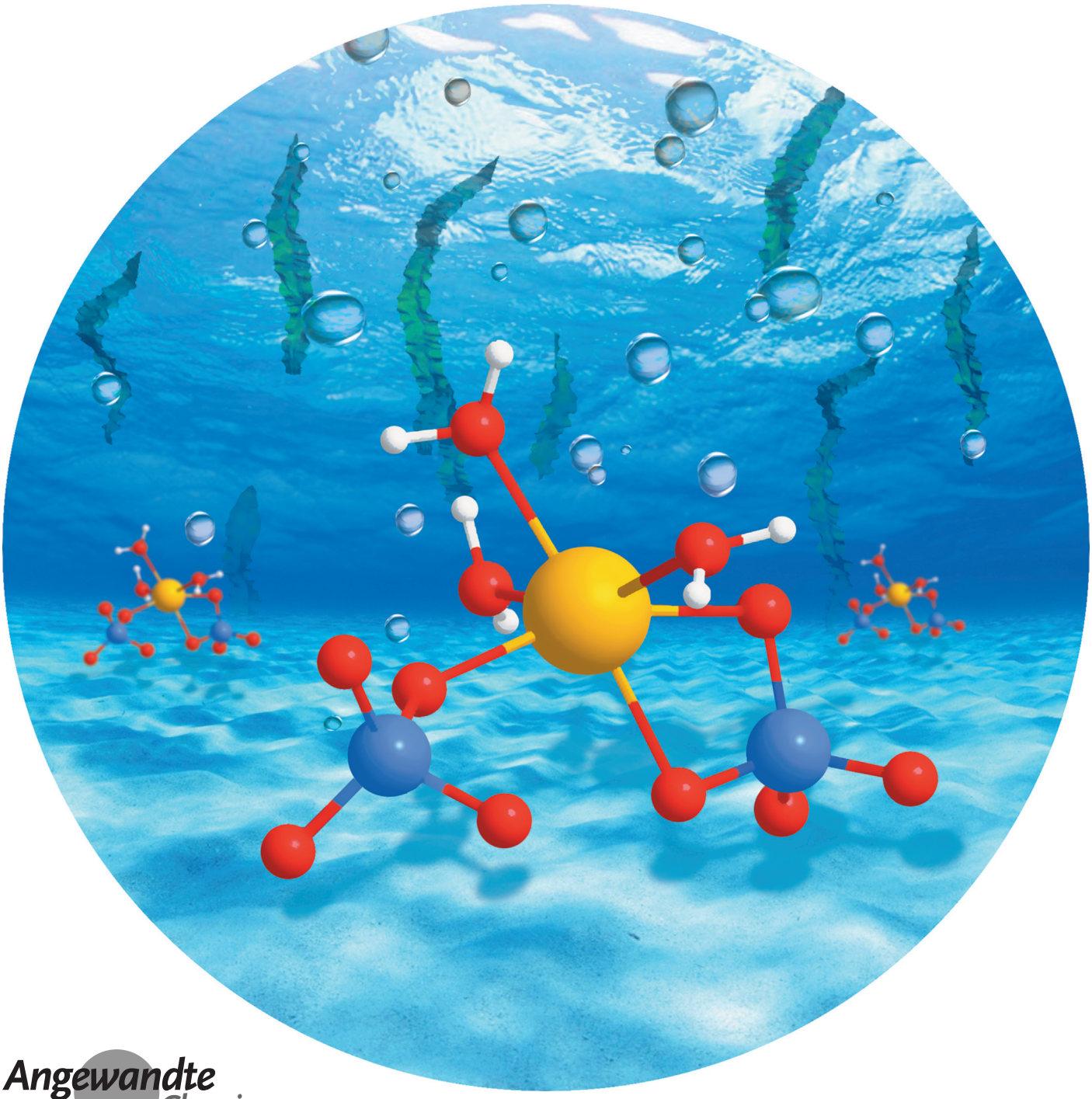

Abstract: *Although FeO_4^{2-} (ferrate(IV)) is a very strong oxidant that readily oxidizes water in acidic medium, at pH 9–10 it is relatively stable (<2% decomposition after 1 h at 298 K). However, FeO_4^{2-} is readily activated by Ca^{2+} at pH 9–10 to generate O_2. The reaction has the following rate law: $d[O_2]/dt = k_{Ca}[Ca^{2+}][FeO_4^{2-}]^2$. ^{18}O-labeling experiments show that both O atoms in O_2 come from FeO_4^{2-}. These results together with DFT calculations suggest that the function of Ca^{2+} is to facilitate O–O coupling between two FeO_4^{2-} ions by bridging them together. Similar activating effects are also observed with Mg^{2+} and Sr^{2+}.*

Plants and cyanobacteria make use of a Mn_4CaO_5 cluster located at the oxygen-evolving center (OEC) of photosystem II (PSII) to carry out water oxidation.[1–4] The protons and electrons obtained from water oxidation are ultimately used to reduce carbon dioxide to carbohydrates. Various multimanganese complexes have been synthesized as structural models of the OEC.[5–10] Notably the recently reported Mn_3CaO4 cluster[7–9] and the Mn_4CaO_4 cluster[10] are closely related to the cubane structure of the OEC. There are also a few studies on the effects of Ca^{2+} and other metal ions on the properties and reactivities of manganese oxo clusters and other model compounds of PSII. For example, the presence Ca^{2+} and other non-redox active metal aqua ions shift the reduction potentials (E^0) of manganese oxo clusters and there is a linear correlation between E^0 and pK_a of the metal ions.[11,12] The catalytic water-oxidation activity of manganese oxides is enhanced by the presence of Ca^{2+}.[13,14] Ca^{2+} is also found to induce the oxidative release of O_2 from a non-heme iron peroxo complex, while other metal ions that are better Lewis acids than Ca^{2+} are not effective.[15]

We are interested to investigate the effects of Ca^{2+} and other Group 2 ions on water oxidation by simple, well-defined molecular metal oxo species, which would facilitate interpretation of kinetic and mechanistic data. Herein we report the effects of Ca^{2+}, Mg^{2+}, and Sr^{2+} on water oxidation at pH 9–10 by K_2FeO_4, which is a very stable black solid at room temperature under moisture-free conditions. Potassium and other metal ferrates have received much attention in recent years because of their potential use as green oxidants in organic synthesis and water treatment.[16]

Although ferrate(VI) (FeO_4^{2-}) is a strong oxidant (E^0 = 2.2 V and 0.72 V at pH 0 and 14, respectively) that readily oxidizes water at low pH,[17] at pH 9–10 it is relatively stable at room temperature.[17] In our hands decomposition of a 1 mM solution is less than 2% in 1 h at pH 9–10 at 298 K, as monitored by UV/Vis spectrophotometry. At pH > 9 ferrate(VI) exists predominantly as the FeO_4^{2-} ion, since the pK_a of $HFeO_4^-$ is 7.3.[16] However, upon adding a few equivalents of Ca^{2+} to K_2FeO_4 in water at pH 10 and 298 K, O_2 evolution readily occurred, as monitored by a gas chromatography–thermal conductivity detector (GC-TCD; Figure 1, Table S1). The rate and the amount of O_2 increase with increasing FeO_4^{2-} concentration (Figure 1a) and increasing Ca^{2+} concentration (Figure 1b), but saturation behavior occurs above

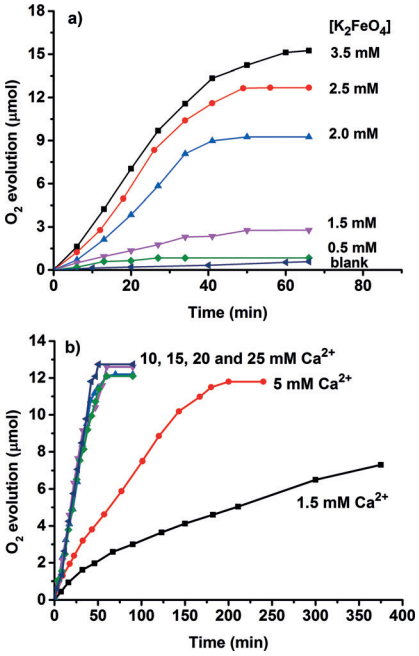

Figure 1. Plots of O_2 evolution (determined by GC) versus time for Ca^{2+}-induced oxygen generation by K_2FeO_4 at initial pH 10, T = 298 K. a) Effects of $[K_2FeO_4]$; $[Ca(OTf)_2]$ = 15 mM. b) Effects of $[Ca(OTf)_2]$; $[K_2FeO_4]$ = 2.5 mM.

4 equivalents of Ca^{2+}. A maximum yield of 85% was obtained after 1 h. The yields were calculated based on Equation (1). An orange precipitate of $Fe(OH)_3$ was observed as the reaction proceeded. Similar yields and rates were obtained when the reaction was carried out at pH 9.0 (Table S1 and Figure S1 in the Supporting Information). In the absence of Ca^{2+} only a trace amount of O_2 was observed after 1 h (<2%). Mg^{2+} and Sr^{2+} showed similar activating effects on oxygen generation by FeO_4^{2-} at pH 9–10, with maximum O_2 yields of 73% and 90%, respectively (Table S1 and Figure S2–5).

According to Equation (1) the pH of the solution should

$$4\,FeO_4^{2-} + 10\,H_2O \rightarrow 4\,Fe(OH)_3 + 3\,O_2 + 8\,OH^- \quad (1)$$

increase during water oxidation. Indeed when 2.5 mM of K_2FeO_4 was mixed with 15 mM Ca^{2+} the pH of the solution increased from 10.0 to 11.6 after 1 h. To minimize pH changes which could affect the rate of the reaction, the kinetics of M^{2+}-induced water oxidation were also investigated at relatively low FeO_4^{2-} concentrations (0.1–0.5 mM); under these conditions the pH of the solutions increased by no more than 0.2. At such low FeO_4^{2-} concentrations the amount of O_2 evolved could not be accurately determined by GC, instead O_2 was continuously monitored by a Clark-type electrode.

[*] Dr. L. Ma, Dr. W. W. Y. Lam, Dr. P. K. Lo, Dr. K.-C. Lau, Prof. T.-C. Lau
Department of Biology and Chemistry and Institute of Molecular Functional Materials, City University of Hong Kong
Tat Chee Avenue, Kowloon Tong, Hong Kong (China)
E-mail: kaichung@cityu.edu.hk
bhtclau@cityu.edu.hk

Supporting information for this article is available on the WWW under http://dx.doi.org/10.1002/anie.201510156.

Figure 2 shows the effects of FeO_4^{2-} concentration on Ca^{2+}-induced oxygen generation by FeO_4^{2-} at pH 10. The experiments were carried out at nearly constant ionic strength using an excess of Ca^{2+} (20 mM). A plot of the initial rate vs. $[FeO_4^{2-}]^2$ gives a straight line (Figure 2b). The effects of Ca^{2+}

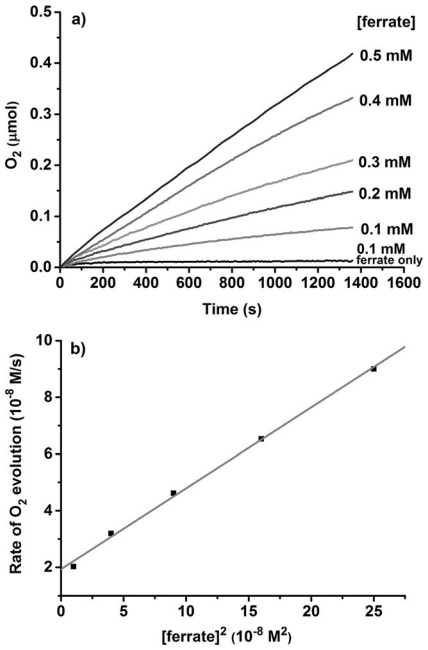

Figure 2. a) Effects of FeO_4^{2-} concentration on Ca^{2+}-induced oxygen generation (O_2 determined by Clark electrode) by K_2FeO_4 at pH 10 and 298 K. $[Ca^{2+}] = 20$ mM. b) Plot of initial rate of O_2 evolution versus $[FeO_4^{2-}]^2$. Slope = 0.29, y-intercept = 1.93×10^{-8}, $r^2 = 0.996$.

concentration on oxygen generation under an excess of FeO_4^{2-} (2.5 mM) were also investigated (Figure 3a). A plot of initial rate versus Ca^{2+} concentration gives a straight line (Figure 3b). These result are in accordance with the rate law: $d[O_2]/dt = k_{Ca}[Ca^{2+}][FeO_4^{2-}]^2$. The same rate law was observed when Mg^{2+} or Sr^{2+} was used to activate FeO_4^{2-} (Figure S6–12). The rate constants ($M^{-2}s^{-1}$) follow the order $k_{Mg}(0.138 \pm 0.017) > k_{Ca}(0.129 \pm 0.014) > k_{Sr}(0.09 \pm 0.018)$, this order is the same as that of their Lewis acidity (pK_a of Mg^{2+}, Ca^{2+} and Sr^{2+} are 11.2, 12.7, and 13.2, respectively).[18] However, the differences in the rate constants are rather small, despite a difference in two pK_a units among these metal ions. When Ba^{2+} (pK_a 13.4) was added to FeO_4^{2-} at pH 9–10, a precipitate of $Ba[FeO_4]$ was immediately formed, and no O_2 evolution could be observed. Other M^{2+} aqua ions such as Co^{2+}, Ni^{2+}, and Zn^{2+} gave $M(OH)_2$ precipitates at pH 9–10.

The effects of Ca^{2+} on FeO_4^{2-} in water has also been monitored by UV/Vis spectrophotometry (Figure S13). There is a gradual appearance of a broad absorption around 400 nm, consistent with the formation of $Fe(OH)_3$. Similar changes were observed when Sr^{2+} or Mg^{2+} was used instead of Ca^{2+}.

To determine the source of O atoms in O_2 evolved, ^{18}O-labeling experiments were performed. FeO_4^{2-} exchanges its O atoms with H_2O, and a rate constant of 1.37×10^{-3} s^{-1} at 273 K was reported.[17a] In our hands we obtained a first-order rate constant of $(2.18 \pm 0.27) \times 10^{-3}$ s^{-1} ($t_{1/2} = 5.3$ min) at 298 K for

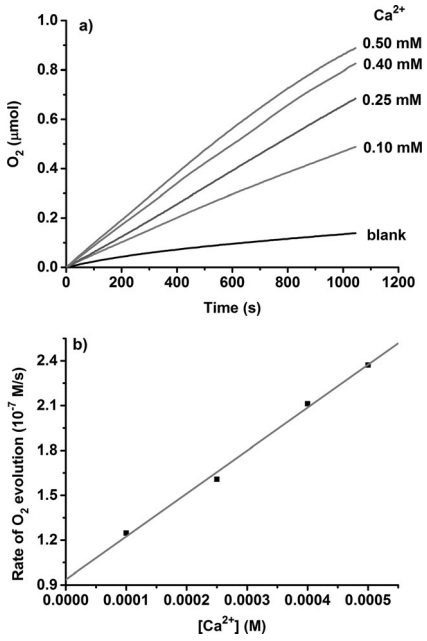

Figure 3. a) Effects of Ca^{2+} concentration on oxygen generation (O_2 determined by Clark electrode) by K_2FeO_4 at pH 10. $[FeO_4^{2-}] = 2.5$ mM. b) Plot of initial rate of O_2 evolution vs. $[Ca^{2+}]$. Slope = 2.87×10^{-4}, y-intercept = 9.37×10^{-8}, $r^2 = 0.993$.

O-exchange between $K_2Fe^{16}O_4$ and $H_2{}^{18}O$, using electrospray ionization mass spectrometry (ESI/MS; Table S2 and Figure S14,15). When $K_2Fe^{18}O_4$ was dissolved in $H_2{}^{16}O$ at pH 10 in the presence of 8 mol equivalents of Ca^{2+} at 298 K, the O_2 evolved after 3 min consists of 27.7 % $^{16}O^{16}O$, 19.2 % $^{16}O^{18}O$, and 53.1 % $^{18}O^{18}O$; the relative amount of $^{18}O^{18}O$ decreased with time as a result of O-exchange between FeO_4^{2-} and water (Table S3). On the other hand, when $K_2Fe^{16}O_4/Ca^{2+}$ was dissolved in $H_2{}^{18}O$, the oxygen evolved after 3 min consists of 68.7 % $^{16}O^{16}O$, 6.3 % $^{16}O^{18}O$, and 25.0 % $^{18}O^{18}O$ (Table S4). As expected, the relative amount of $^{18}O^{18}O$ increased with time in this case. These results unambiguously establish that both O atoms in the O_2 evolved come from FeO_4^{2-} (after correcting for O-exchange between FeO_4^{2-} and H_2O during 3 min). The ^{18}O-labeling results, together with the observed second-order dependence of the rate on FeO_4^{2-} concentration, are consistent with a O_2 evolution mechanism that involves O–O coupling between two FeO_4^{2-} bound to a Ca^{2+} ion, as shown in Equations (2)–(3). The iron(IV) species formed after O_2 evolution is expected to undergo rapid disproportionation to give FeO_4^{2-} and $Fe(OH)_3$.[17]

$$2[FeO_4]^{2-} + Ca^{2+} \rightleftharpoons \{Ca[FeO_4]_2\}^{2-} \quad (2)$$

$$\{Ca[FeO_4]_2\}^{2-} \rightarrow \{Ca[FeO_3]_2\}^{2-} + O_2 \quad (3)$$

We and others have previously reported that Fe_2O_3/$Fe(OH)_3$ nanoparticles, either directly used or generated from iron complexes and salts, can catalyze visible-light induced water oxidation by $[Ru(bpy)_3]^{2+}/S_2O_8^{2-}$ at pH 7–9.[19] However, the active intermediate should not be FeO_4^{2-} since in the absence of Ca^{2+} it oxidizes water very slowly in this pH range. Also Ca^{2+} ions did not have any effects on catalytic water

oxidation by this system (Figure S16).

To obtain more insights into the mechanism of Ca^{2+}-induced oxygen generation by FeO_4^{2-}, density functional theory (DFT) calculations have been performed on the reaction between FeO_4Ca and FeO_4^{2-}. As the evolution of O_2 from FeO_4^{2-}/Ca^{2+} occurs in aqueous medium, the solvent effect was treated by a hybrid model which consists of an explicit solvent effect of 13 water molecules surrounding FeO_4Ca and FeO_4^{2-} and an implicit solvent effect by polarizable continuum model (PCM).[20] The $^3[FeO_4]^{2-}$ and $^3[FeO_4Ca]$ species first couple to form a stable quintet intermediate, $^5[FeO_4CaFeO_4{\cdot}13H_2O]^{2-}$ (**^{5}INT1a**) (Scheme 1).

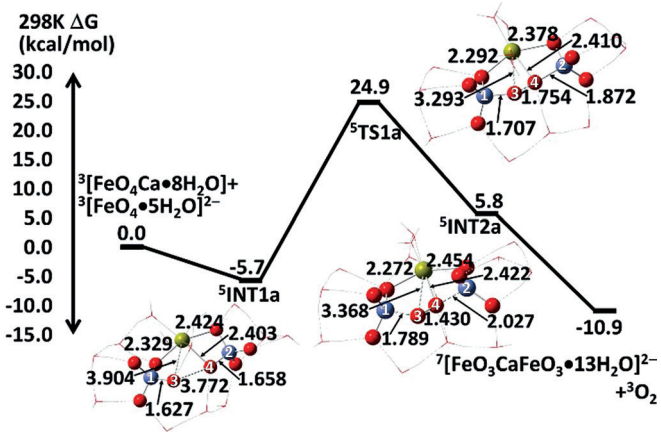

Scheme 1. Quintet potential energy surface for the O_2 evolution from $[FeO_4Ca{\cdot}8H_2O]+[FeO_4{\cdot}5H_2O]^{2-}$ at the B3LYP level using LanL2TZ(f) basis set (Fe) and 6-311++G(d,p) basis set (H, O, and Ca). Relative 298 K Gibbs free energies in water are given in kcal mol^{-1} and selected bond lengths are in Å. O red, Fe purple, Ca green.

In **^{5}INT1a**, the Ca^{2+} has an octahedral coordination environment; it is bonded to three water molecules, two oxo ligands of one FeO_4^{2-} and one oxo ligand of the other FeO_4^{2-}. The electron spin density on each FeO_4^{2-} is fairly even; the Fe metal bears approximately 1.4 electrons and the oxo ligand has approximately 0.2 electrons. This suggests that the **^{5}INT1a** is formed by a direct coupling of $^3[FeO_4{\cdot}5H_2O]^{2-}$ and $^3[FeO_4Ca{\cdot}8H_2O]$ without any significant change in electronic distribution. There is no significant change in Fe–O distances before and after binding to Ca^{2+} (Table S5–7). The **^{5}INT1a** then undergoes O–O coupling between a non-Ca^{2+} bound oxo ligand of one FeO_4^{2-} and a Ca^{2+}-bound oxo ligand of the other FeO_4^{2-} (i.e. between O3 and O4) via **^{5}TS1a** to form **^{5}INT2a**. The O3–O4 distance is significantly shortened from 3.772 Å to 1.754 Å whereas the Fe1–O3/Fe2–O4 bond lengths are slightly elongated by 0.08–0.21 Å in **^{5}TS1a**. The free-energy barrier height ($\Delta G_{298}^{\ddagger}$) of **^{5}TS1a** is 24.9 kcal mol^{-1}. In **^{5}INT2a**, the O3–O4 bond length of 1.430 Å is consistent with a peroxo bond. The **^{5}INT2a** then decomposes into $^3O_2$ and $^7[FeO_3CaFeO_3{\cdot}13H_2O]^{2-}$ with $\Delta G = -16.7$ kcal mol^{-1}; and the electron spin on O3 and O4 become −1.0 while the electron spin on Fe1 and Fe2 are about +2.0. Each of the remaining oxo group bears approximately 0.2 electrons. The **^{5}INT2a** is adiabatically correlated with $^7[FeO_3CaFeO_3{\cdot}13H_2O]^{2-}$ and $^3O_2$.

We have also calculated the potential energy surface for O–O coupling through the $^3[FeO_4CaFeO_4{\cdot}13H_2O]^{2-}$ (**^{3}INT1a**) intermediate (Scheme S1), however in this case the barrier is much higher (46.1 kcal mol^{-1}).

The reaction mechanisms for O_2 evolution from $FeO_4Mg + FeO_4^{2-}$ and $FeO_4Sr + FeO_4^{2-}$ are similar to that of $FeO_4Ca + FeO_4^{2-}$. The $\Delta G_{298}^{\ddagger}$ (kcal mol^{-1}) for O_2 evolution from the three metal ions follow the order $Mg^{2+}(20.4) < Ca^{2+}(24.9) < Sr^{2+}(28.7)$, which is the same as the experimentally determined order.

In conclusion, we have demonstrated that the Group 2 metal aqua ions Mg^{2+}, Ca^{2+}, and Sr^{2+} readily activate the FeO_4^{2-} ion at pH 9–10 to generate O_2. Experimental and DFT calculations suggest that the reaction goes through a $\{M[FeO_4]_2\}^{2-}$ intermediate in which the two FeO_4^{2-} ions are bridged by M^{2+}. The M^{2+} appears to play mainly a structural role that brings the two FeO_4^{2-} ions together to facilitate O–O coupling between them (I2M mechanism[21]) to generate a peroxo species. The observed similar rate constants and calculated $\Delta G_{298}^{\ddagger}$ for water oxidation activated by the three different metal ions suggests that there is little electronic effect of the M^{2+} ions. The Fe–O distances in free and M^{2+}-bound FeO_4^{2-} are also very similar. The proposed mechanism is similar to oxygen generation by FeO_4^{2-} in acidic medium, in which the FeO_4^{2-} is first protonated followed by spontaneous condensation to give an oxo-bridged diferrate, which then undergoes O–O coupling.[17b] Oxygen generation by ferrate(V) at pH around 5–8 may be represented by Equations (4)–(6). At lower pH ferrate(VI) may undergo di- and tri-protonation followed by condensation ($H_3Fe^{VI}O_4$, $pK_1 = 1.5$, $pK_2 = 3.5$, $pK_3 = 7.2$).[16b] At pH > 9 μ-oxo species cannot form. However, we show in this work that the Group 2 ions can also bring the two ferrates together to facilitate O–O coupling.

$$[FeO_4]^{2-} + H^+ \rightleftharpoons [FeO_3(OH)]^- \quad (4)$$

$$2[FeO_3(OH)]^- \rightarrow [O_3Fe\text{-}O\text{-}FeO_3]^{2-} + H_2O \quad (5)$$

$$[O_3Fe\text{-}O\text{-}FeO_3]^{2-} \rightarrow [O_2Fe\text{-}O\text{-}FeO_2]^{2-} + O_2 \quad (6)$$

Acknowledgements

This work was supported by Hong Kong University Grants Committee (AoE/P-03-08) and the Research Grants Council of Hong Kong (CityU 101612 and CityU 11301514).

Keywords: calcium · dioxygen generation · iron(VI) · Lewis acid

How to cite: *Angew. Chem. Int. Ed.* **2016**, *55*, 3012–3016
Angew. Chem. **2016**, *128*, 3064–3068

[1] J. P. McEvoy, G. W. Brudvig, *Chem. Rev.* **2006**, *106*, 4455–4483.
[2] J. Barber, *Chem. Soc. Rev.* **2009**, *38*, 185–196.
[3] Y. Umena, K. Kawakami, J. R. Shen, N. Kamiya, *Nature* **2011**, *473*, 55–60.
[4] J. Yano, V. Yachandra, *Chem. Rev.* **2014**, *114*, 4175–4205.

[5] C. S. Mullins, V. L. Pecoraro, *Coord. Chem. Rev.* **2008**, *252*, 416 – 443.
[6] G. C. Dismukes, R. Brimblecombe, G. A. N. Felton, R. S. Pryadun, J. E. Sheats, L. Spiccia, G. F. Swiegers, *Acc. Chem. Res.* **2009**, *42*, 1935 – 1943.
[7] J. S. Kanady, E. Y. Tsui, M. W. Day, T. Agapie, *Science* **2011**, *333*, 733 – 736.
[8] S. Mukherjee, J. A. Stull, J. Yano, T. C. Stamatatos, K. Pringouri, T. A. Stich, K. A. Abboud, R. D. Britt, V. K. Yachandra, G. Christou, A. Affiliations, *Proc. Natl. Acad. Sci. USA* **2012**, *109*, 2257 – 2262.
[9] J. S. Kanady, P. H. Lin, K. M. Carsch, R. J. Nielsen, M. K. Takase, W. A. Goddard III, T. Agapie, *J. Am. Chem. Soc.* **2014**, *136*, 14373 – 14376.
[10] C. X. Zhang, C. H. Chen, H. X. Dong, J. R. Shen, H. Dau, J. Q. Zhao, *Science* **2015**, *348*, 690 – 693.
[11] E. Y. Tsui, R. Tran, J. Yano, T. Agapie, *Nat. Chem.* **2013**, *5*, 293 – 299.
[12] E. Y. Tsui, T. Agapie, *Proc. Natl. Acad. Sci. USA* **2013**, *110*, 10084 – 10088.
[13] M. M. Najafpour, T. Ehrenberg, M. Wiechen, P. Kurz, *Angew. Chem. Int. Ed.* **2010**, *49*, 2233 – 2237; *Angew. Chem.* **2010**, *122*, 2281 – 2285.
[14] M. Wiechen, I. Zaharieva, H. Dau, P. Kurz, *Chem. Sci.* **2012**, *3*, 2330 – 2339.
[15] S. Bang, Y. M. Lee, S. Hong, K. B. Cho, Y. Nishida, M. S. Seo, R. Sarangi, S. Fukuzumi, W. Nam, *Nat. Chem.* **2014**, *6*, 934 – 940.
[16] a) V. K. Sharma, R. Zboril, R. S. Varma, *Acc. Chem. Res.* **2015**, *48*, 182 – 191; b) V. K. Sharma, *Coord. Chem. Rev.* **2013**, *257*, 495 – 510; c) V. K. Sharma, *J. Environ. Manage.* **2011**, *92*, 1051 – 1073.
[17] a) H. Goff, R. K. Murmann, *J. Am. Chem. Soc.* **1971**, *93*, 6058 – 6065; b) R. Sarma, A. M. Angeles-Boza, D. W. Brinkley, J. P. Roth, *J. Am. Chem. Soc.* **2012**, *134*, 15371 – 15386; c) Y. Lee, R. Kissner, U. Gunten, *Environ. Sci. Technol.* **2014**, *48*, 5154 – 5162.
[18] S. J. Hawkes, *J. Chem. Educ.* **1996**, *73*, 516 – 517.
[19] a) G. Chen, L. J. Chen, S. M. Ng, W. L. Man, T. C. Lau, *Angew. Chem. Int. Ed.* **2013**, *52*, 1789 – 1791; *Angew. Chem.* **2013**, *125*, 1833 – 1835; b) D. Hong, S. Mandal, Y. Yamada, Y. M. Lee, W. Nam, A. LIobet, S. Fukuzumi, *Inorg. Chem.* **2013**, *52*, 9522 – 9531; c) Q. J. Xiang, G. Chen, T. C. Lau, *RSC Adv.* **2015**, *5*, 52210 – 52216.
[20] a) S. Miertuš, E. Scrocco, J. Tomasi, *Chem. Phys.* **1981**, *55*, 117 – 129; b) S. Miertuš, J. Tomasi, *Chem. Phys.* **1982**, *65*, 239 – 245.
[21] X. Sala, S. Maji, R. Bofill, J. García-Antón, L. Escriche, A. Llobet, *Acc. Chem. Res.* **2014**, *47*, 504 – 516.

Received: November 1, 2015
Published online: January 22, 2016

